Long term self-cleaning and photocatalytic performance of anatase added mortars exposed to the urban environment

Maria Vittoria Diamanti [a], Riccardo Paolini [b,*], Marta Rossini [a], Aysegul Basak Aslan [a], Michele Zinzi [c], Tiziana Poli [b], Maria Pia Pedeferri [a]

[a] *Politecnico di Milano, Dipartimento di Chimica, Materiali e Ingegneria Chimica "G. Natta", Via Mancinelli 7, 20131 Milan, Italy*
[b] *Politecnico di Milano, Department of Architecture, Built Environment and Construction Engineering, Milan, Italy*
[c] *ENEA – UTEE-ERT Italian National Agency for New Technologies, Energy and Sustainable Economic Development, Rome, Italy*

Received 21 July 2015
Received in revised form 31 July 2015
Accepted 7 August 2015
Available online 13 August 2015

1. Introduction

The use of TiO_2-modified building materials has been constantly expanding in the last decade, especially in European countries, to exploit their photoactivated depolluting and self-cleaning properties [1–4]. This diffusion is also driven by a growing need for building envelope materials with high solar reflectance and thermal emittance [5–8], or retro-reflective materials that applied onto façades could reflect the solar direct radiation towards the sky, and not towards other buildings [9,10]. In fact, these materials could help to preserve the aesthetics of the building skin, reduce and reshape the energy needs and indoor comfort conditions of buildings [11–14], also contributing to the mitigation of urban

* Corresponding author at: Via Ponzio 31, 20133 Milano, Italy.
E-mail address: riccardo.paolini@polimi.it (R. Paolini).

microclimates [15]. Consider for instance the cooling loads: for the same building, within urban areas the cooling need is in average 13% more than outside the city [16]. This, may yield to an increase by 7% of CO_2 equivalent annual emissions, computed for a reference building in Northern Italy [17]. However, the possible cooling savings and mitigation potential may be compromised by aging [18,19], which is due to the combined action of weathering, soiling, biological growth, and mechanical stress [20–23]. In addition, cleaning techniques do not seem effective to restore the initial reflectance of porous materials such as roofing tiles [24].

The major cause of staining and color variation of building surfaces, reducing the initial solar reflectance, is the accumulation of soot, mainly originated from atmospheric aerosol pollutants such as nitric oxides, carbon based substances and volatile organic compounds [25,26]. Such substances can dissolve in water (i.e., rain and surface condensation) and/or penetrate inside the pores of façade materials (e.g., bricks, claddings, mortars), affecting the aes-thetics and reflectance of the façade, and contributing to the phys-ical degradation of external surfaces [27–29].

In this respect, self-cleaning and photocatalytic materials have the added value of a potential prolonged maintaining of their optical performance in spite of soot and particulate matter deposition [30,31], and of mitigating atmospheric pollution [32–35]. The principle on which photoactive materials rely is the activation of a semiconductor through energy provided by light of different wavelength depending on the semiconductor bandgap, generally in the range of near UV or blue visible light. This generates electron/hole couples across the semiconductor bandgap – which in turn induce the formation of highly reactive species, among which hydroxyl radicals play a vital role [36,37]. In fact, these species are then responsible for redox reactions that degrade inorganic and organic compounds adsorbed on the material surface – e.g., volatile organic compounds (VOCs) or NO_x present in the atmosphere. On the other side, the adsorption of the same hydroxyl radicals forms a hydroxylated surface layer that increases hydrophilicity [36,38–40]. The combination of these two mechanisms leads to a self-cleaning effect, where the former helps degrading functional groups by which pollutants adhere to a surface, while the latter spreads water homogeneously over the surface, carrying away particulate matter and degraded contaminants [41–43].

During the last years, many studies have investigated the photocatalytic activity of TiO_2 applied on different materials, in the field of new construction technologies and for cultural heritage preservation [44–47]. Yet, although TiO_2-functionalized building materials are already commercially available, a full appraisal of their long-term performance in use conditions is still missing. Only a few studies in the literature go beyond the measurement of the photodegradation of a given pollutant, or their self-cleaning efficiency in laboratory conditions, and actually propose a long-term approach to this issue [27,40,48–50].

Literature data show that, after aging, the ability of TiO_2 coatings to remove NO_x from air and their self-cleaning ability decreased compared with the initial performance [48]. The loss of TiO_2 efficiency was associated to natural aging after outdoor exposure, especially in the case of coatings subjected to climatic conditions [50,51]. Environmental stress may cause particles detachment and thickness reduction of the coating, owing to the degradation of the coating binder and consequent detachments, as well as a partial deactivation due to the adsorption of pollutants or reaction products of the photocatalytic processes [48,52].

This study reports a two-year campaign of natural exposure in Milano, Italy, of photoactive and non-photoactive fiber-reinforced mortars with different surface finishing, analyzing the evolution of lightness, solar reflectance, porosity and photoactivity of materials.

2. Experimental

2.1. Materials

The materials tested in this work are commercial fiber-reinforced mortars, which are used for rain-screen façade panels as well as pre-cast thermally insulated panels, for new construc-tions and refurbishment interventions.

For the tests performed in this work, samples composition is reported in Table 1; all mortars were cast with a cement:sand:water ratio of 1:2:0.56. A first fast stirring step was performed to mix water, cement, pigments and chemical additives, followed by a slower mixing where sand and glass fibers were added. The mixture was then extruded on a continuous polystyrene sheet with 8 mm of mortar thickness. Curing in a controlled temperature (25 °C) and relative humidity (65%) chamber lasted 24 h, after which the fiber-reinforced mortar was cut in 100 mm × 100 mm samples, and eventually surface finished if required. Samples with both standard composition and the addition of anatase (a mixture of 2% aqueous suspension and 3% nanopowder, optimized in previ-ous works [53]) were used. Tests were performed on mortars with two different surface finishing conditions, sandblasted and smooth, in order to evaluate the effect of different surface roughness on the self-cleaning performance. XRD (X-ray diffraction) analyses were carried out on the materials used in order to examine the composition of the mortars under investigation.

2.2. Outdoor natural exposure

The selected samples were exposed to the urban environment, on a rooftop of Politecnico di Milano – approx. height 25 m, unsheltered – for a period of two years starting October 2012, in correspondence with the winter activation of buildings heating systems.

Samples were positioned facing both north and south with multiple inclinations (vertical, horizontal, tilted by 45°, and vertical-sheltered) to have a wider understanding of the influence of different microclimates (irradiation, wind, rain), which is also connected with the wetting extent during rain events and therefore with the onset of the superhydrophilicity and self-cleaning (Fig. 1). Samples were sealed with silicone on the four edges and on the back to make them waterproof, and fastened to the racks.

All samples were labeled with reference to their characteristics:

- Sample composition (S: standard, T: with TiO_2).
- Finishing (L: smooth, S: sandblasted).
- Exposure orientation (N: north, S: south).
- Inclination: (H: horizontal, S: vertical sheltered, I: inclined by 45°, V: vertical unsheltered).

Three replicates were originally exposed for each combination of these conditions, for a total of 96 samples. After the first year, one sample per type was withdrawn to perform accelerated photocatalysis tests; consequently the exposure continued with two specimens per type.

Table 1
Composition of mortar samples used in the experimental work.

Composition	Dosage	
Portland cement Roccabianca 42.5R	555 kg/m^3	
Silica sand	1110 kg/m^3	
Water	311 kg/m^3	
Expansive agent Stabilmac	33 kg/m^3	6%
Waterproof additive	22 kg/m^3	4%
Glass fibers	20 kg/m^3	3.6%
Antifoam agent	1 kg/m^3	0.1%

Fig. 1. Samples exposed on the rooftop of Politecnico di Milano, oriented south (a), north right after a snowfall (b), and during colorimetry measurements (c).

2.2.1. Color measurements

The evaluation of self-cleaning behavior was based on monitoring the variations in color and solar reflectance of the exposed samples. A portable Vis spectrophotometer CM-2500d by Konica Minolta was used to monitor color variations periodically – on a bi-weekly basis in the first period of exposure, where more marked variations were expected, then on a monthly basis. Data were processed in the CIELab color space, defined by the Commission Internationale de l'Éclairage as composed by three color coordinates: L^*, brightness; a^*, hues from red to green; and b^*, hues from yellow to blue. Attention was focused in monitoring variations of ΔL^* (gray) and Δb^* (yellow) as representative of dirt accumulation on the surface. Measurements were taken in three different points for each sample, in order to minimize the possible errors due to random variables such as climatic factors or sample surface heterogeneities.

2.2.2. UV–Vis–NIR spectrometry

Solar spectral reflectance was measured with a Perkin Elmer Lambda 950 UV–Vis–NIR spectrometer equipped with a 150 mm diameter integrating sphere. One measurement per sample was performed in the 300–2500 nm wavelength range with a spectral resolution of 5 nm, and the average curve was then computed. Broadband values were computed according to ISO 9050 [54], with visible range defined between 380 and 780 nm. The samples were measured before the exposure, and retrieved, measured and re-exposed at 6, 12, and 24 months of natural aging.

2.2.3. Mercury intrusion porosimetry

Before and after natural aging, porosity, pore size distribution and permeability of the mortars were determined by means of mercury intrusion porosimetry (MIP), by means of a Micromeritics AutoPore IV 9500 series mercury intrusion porosimeter.

2.3. Accelerated cleaning

Horizontal samples were subjected to accelerated UV exposure, in order to stimulate photocatalytic degradation of soot accumulated on the surface. This was performed under artificial irradiation provided by an Osram Vitalux 300 W lamp, simulating the sunlight spectrum, positioned so as to obtain UV intensity of 1000 μW/cm^2. The exposure test lasted 18 days and during the whole period the color of samples was periodically monitored, evaluating possible changes in their lightness and yellowing. Once a week samples were temporarily removed from the light source, rinsed with running water, and let dry. Samples color was recorded before and after every rinse.

2.4. Accelerated photocatalysis tests

The photoactivity of investigated materials was evaluated through accelerated photocatalysis tests in various phases of their service life. The tests consisted of monitoring the discoloration of a magenta organic dye, rhodamine B (RhB), deposited on the mortars surface, by means of color analyses, which were performed by using the previously described portable spectrophotometer. As the dye color is due to absorption by its chromophore groups, discoloration is generally considered as representative of dye degradation [55–57].

According to UNI 11259 standard [58], the mortars were sprayed with an aqueous RhB solution with concentration 0.05 ± 0.005 g/l and allowed to dry for 24 h. Subsequently, the sam-ples were exposed to artificial sunlight, provided by the same apparatus used for accelerated cleaning, setting a UV irradiation of 375 μW/cm^2. The color was measured every 1 h in the first 6 h irradiation and at the end of the 24 h test, and the a^* coordinate, related to red hues, was used to evaluate the dye discoloration extent. In particular, a material is considered photoactive only if the following requirements are satisfied:

$$R_4 > 20\% \text{ and } R_{26} > 50\% \quad (1)$$

where:

$$R_4 = \frac{a^*(0) - a^*(4)}{a^*(0)} \times 100 \quad (2)$$

$$R_{26} = \frac{a^*(0) - a^*(26)}{a^*(0)} \times 100 \quad (3)$$

Given $a^*(0)$ the value of a^* at time 0 before irradiation, $a^*(4)$ its value after 4-hour irradiation, and $a^*(26)$ the value after 26-hour irradiation.

Photocatalysis tests were performed on freshly prepared mortars, on naturally aged materials after 1 and 2 years of outdoor exposure, and naturally aged materials after the accelerated cleaning procedure.

3. Results and discussion

3.1. Characterization of freshly prepared mortars

XRD analyses performed on both photoactive and standard mortars show a high intensity peak at 29° that corresponds to the presence of calcite, together with silica in quartz form (relevant peaks: 27°, 36.5°, 55°) and calcium silicates, whose peaks mostly overlap with previous phases. Moreover, at 25° it is possible to observe the main diffraction peak of anatase, which is clearly present on the photoactive sample, but not on the non-photoactive one (Fig. 2).

3.2. Outdoor natural exposure

The results of the exposure tests and the comparison between different materials and conditions of exposure are reported in Fig. 3, where each point is an average of 9 measurements (3

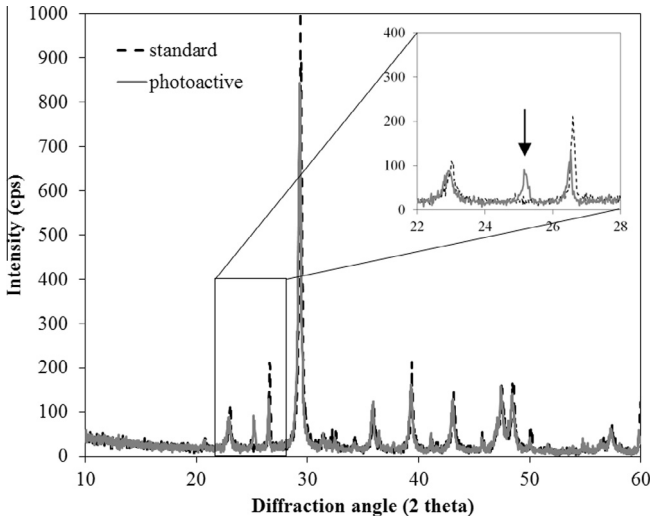

Fig. 2. X-ray diffraction peaks of standard and photoactive mortar samples. Inset: zoom of main anatase peak at 25.2°.

samples per type, 3 measurements on each sample). First of all, it is important to notice a higher initial lightness of photoactive mortars, whose L^* values are 92.7 ± 0.1 (smooth) and 89.1 ± 0.1 (sandblasted) against 89.5 ± 0.1 (smooth) and 86.0 ± 0.1 for standard ones, respectively. Moreover, an evident effect of photoactivity over the long term was observed; in fact, all photoactive samples present a lower – or at least comparable – lightness decrease with respect to standard formulations. From Fig. 3a it is possible to observe that the extent of soiling depends on mortars positioning: horizontally exposed samples (TLSH) are subject to the heaviest color variation, followed by the 45° tilted ones (TLSI), while vertically exposed surfaces – both sheltered (TLSS) and unsheltered (TLSV) – better maintain their original color. As these materials are generally used as rain-screen façade panels, the vertical exposure (sheltered or not) is the most likely condition of practical use. Horizontal exposure was intended to provide a "worst condition" case, representative for solar shading devices or construction details such as the windowsill or drip caps. Therefore, the following considerations will focus on the most interesting case of vertical and sheltered samples.

Exposure orientation also plays a crucial role in determining the amount of particulate matter deposition onto the surface of specimens. Photoactive samples facing north tend to experience a more significant decrease in lightness, mainly due to the fact that they are less exposed to solar irradiation, which reduces the extent of photoactivation (Fig. 3b).

Fig. 3c reports the overall lightness variations, ΔL^*, observed on smooth and sandblasted samples, with both photoactive and standard composition, vertically exposed facing south, while Fig. 3d also includes a comparison between sheltered and unsheltered exposure conditions. After 2 years of natural aging, the maximum decrease in lightness exhibited by photoactive smooth samples is 0.19, while in the case of standard samples the maximum decrease amounts to 1.46. Considering common interpretations of color measurements, which identify a $\Delta L^* = 1$ as threshold for human

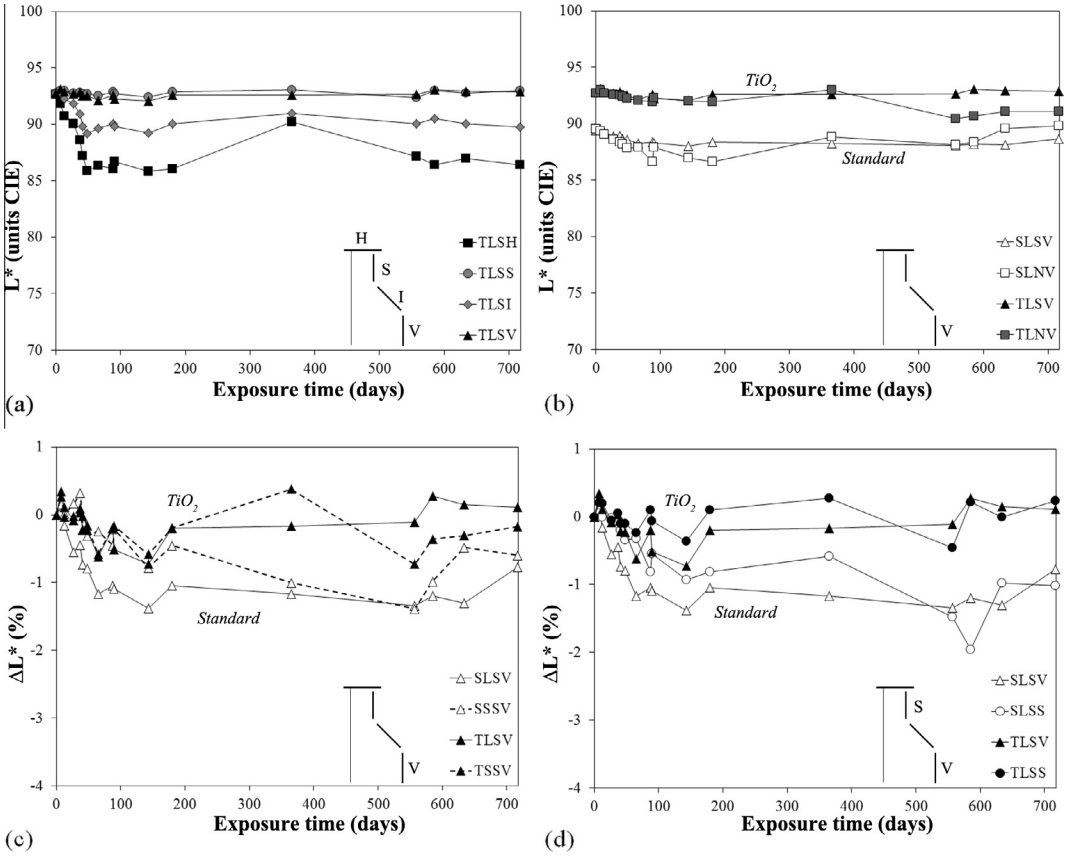

Fig. 3. Lightness (a and b) and lightness percent variation (c and d) recorded on mortars during the two-year exposure. (a) South-exposed photoactive smooth mortars (TLS) oriented in different positions: horizontal (H), sheltered (S), 45° inclined (I) and vertical (V). (b) Photoactive (T) and standard (S) mortars facing north (N) or south (S) on vertical (V) orientation. (c) Photoactive (T) and standard (S) mortars, comparison between smooth (L) and sandblasted (S) surface finishing on vertical (V) orientation. (d) South-exposed photoactive (TLS) and standard smooth (SLS) mortars, effect of sheltering (S) on vertical (V) samples.

Table 2
Mercury intrusion porosimetry results for standard and photoactive smooth mortars: comparison of porosity before and after 2 years of environmental exposure.

Parameters	Standard		Photoactive	
	Before	After	Before	After
Total pore area [m^2/g]	4.30	5.26	5.94	9.55
Average pore radius [μm]	0.050	0.030	0.053	0.024
Porosity [%]	21.6	16.5	28.4	22.6
Characteristic pore length [μm]	0.75	0.59	0.56	0.32
Tortuosity	26.92	46.37	32.35	77.28

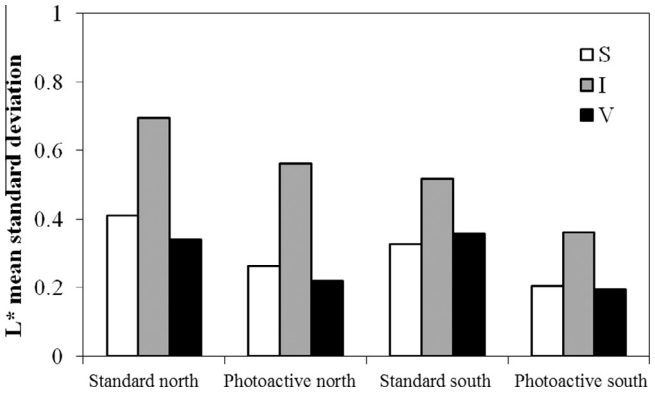

Fig. 4. Standard deviation of lightness measurement over the whole exposure duration on sheltered (S), inclined (I) and vertical (V) specimens.

eye perception, both variations can be considered small, but only that recorded on photoactive samples can be regarded as negligible [40]. When considering sandblasted mortars, a larger variability is introduced in the increased surface roughness, which in general tends to retain a larger quantity of atmospheric soot – as demonstrated by slightly larger ΔL^* observed in the majority of cases with respect to smooth samples, but the trend in smaller lightness variation on photoactive mortars is still maintained.

In this respect, it is possible to observe that on sandblasted specimens, in the long term, water tends to penetrate more easily into pores, carrying particulate matter inside the material and partially filling the open pores. This gives a double effect of increased soiling – and thus, decreased lightness – and decreased porosity, as proved by MIP measurements performed on specimens after the 2-year environmental exposure (Table 2).

Table 2 Mercury intrusion porosimetry results for standard and photoactive smooth mortars: comparison of porosity before and after 2 years of environmental exposure.

Pristine photoactive mortars are characterized by a larger total pore area which causes a higher overall porosity, probably due to a lower compaction degree, while the average pore size is comparable in both materials, which indicates an increase in the number of pores rather than in their size [59]. Water absorption is closely related to the open porosity: the maximum water absorption is related to the total interconnected pore volume of the material, while the rate of water absorption is a measure of the capillary forces exerted by the pore structure causing fluids to be drawn into the body of the material [60]. TiO_2 not only modifies the material structure, but also its chemistry, producing changes in affinity to water of pores surfaces when subjected to UV irradiation [43].

After aging, a reduction of overall porosity and of average pore size was recorded, together with an increase in pore area: this combined effect can be ascribed to the accumulation of particulate matter that blocks the material pores, reducing pore volume while leaving smaller pores that account for a lager total surface. To support this, an increase in tortuosity is also observed, which may yield to an increase in capillary transport within porous media [61].

Yet, differences are not limited to the absolute value of lightness variation, which is itself an important element of evaluation to assess the beneficial effect of anatase addition to mortars formulation. Another crucial element emerged from data analysis is the higher homogeneity of photoactive mortars surfaces, whose appearance is more uniform. In this respect, a first consideration is related to border effects: in fact, soiling conditions at the edges of the samples are not representative, as acknowledged in environmental exposure practice [62]. This border effect, which may be due to a series of phenomena – from the different accumulation and run-off of water on a discontinuity to the presence of silicon – is present on both standard and photoactive samples, and the corresponding area was not considered for analyses in the course of this work. On the other hand, on standard mortars an area affected by detachments and leaching is clearly visible at the bot-tom of the sample, which was much less observed on TiO_2-containing mortars.

Apart from mere visual observations, the claimed improvement in surface homogeneity and integrity was further investigated by analyzing the standard deviations of color measurement. As mentioned in the experimental section, for each material and exposure condition, three samples were used and three color measurements were performed on each sample. Therefore, each single lightness value reported in previous figures is the expression of a mean value over 9 measurements. Along the two years of exposure, 17 measurements were performed at different times. Fig. 5 reports the standard deviation of lightness values on a total of 9×17 measurements, i.e., on a statistically significant population of approximately 150 lightness values measured on a single type of sample throughout the exposure. Horizontal specimens were excluded from the analysis on account of the too large and irregular soiling observed, and of the non-representative character with respect to potential applications of these materials. Data reported in Fig. 4 clearly put in evidence the lower variability of all photoactive specimens with respect to their standard counterparts. Moreover, a larger variability of measurements performed on inclined specimens with respect to vertical ones is noticed in all cases, which pairs with the larger ΔL^* recorded, and can be a consequence of such lar-ger ΔL^* values.

Finally, one last effect observed in the analysis of color coordinates is a pronounced increase in b^* on photoactive samples, as shown in Fig. 5. This was ascribed to the mineralization of organic compounds formerly adsorbed on the surface, which causes surface yellowing due to reaction products remaining on the surface [63], which underlines the fact that TiO_2 containing mortars, in addition to the self-cleaning features, also contribute to the degradation of polluting compounds in the atmosphere.

Coherently with the measured initial lightness, also solar reflectance of photoactive samples was clearly higher than that of standard ones, ensuring from the very beginning a better energy performance of the TiO_2-containing materials. The solar reflectance decreased for all samples after the first 6 months of exposure, almost recovering the initial value at one year of natural aging. Then, at 2 years of aging, it reached approximately the same values that were measured after 6 months. Unlike the lightness assessment, solar reflectance measurements do not show any major difference between anatase containing samples and the standard ones (Fig. 6).

This fluctuation in solar reflectance, common to all specimens, is probably due to the fact that soiled portions of material were rainwashed and eroded from the surface, thus, exposing the pris-tine material underneath, and yielding to a recovery of the initial reflectance.

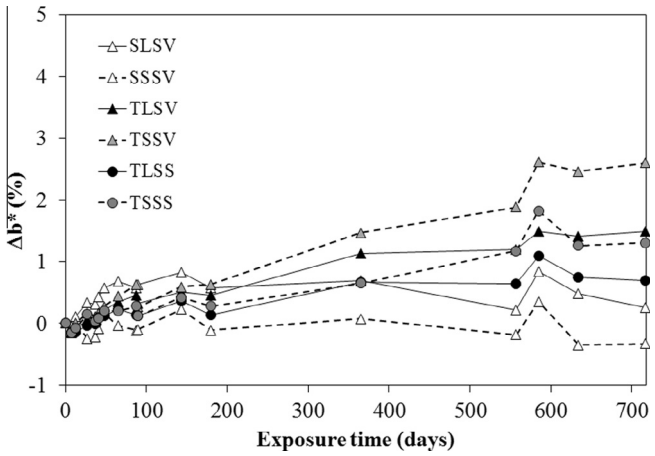

Fig. 5. b^* variation of sheltered and vertical specimens facing south.

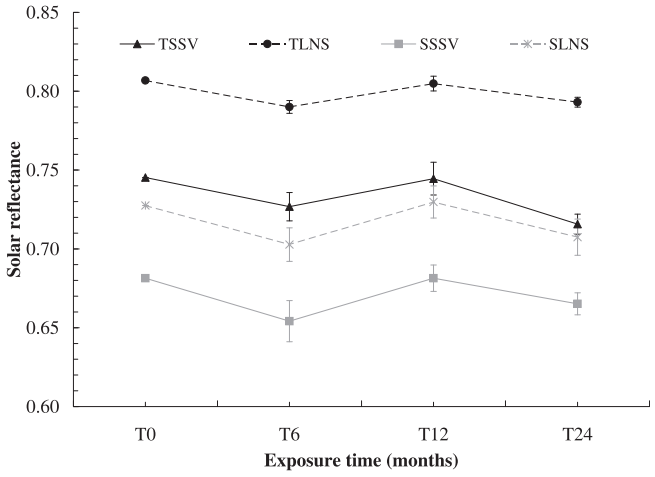

Fig. 6. Solar reflectance (average of the 4 exposure conditions) with exposure time for the smooth and sandblasted TiO_2 and standard samples.

As for the color measurements, also in the case of solar reflectance, anatase containing samples show a smaller standard deviation compared to standard samples. This higher uniformity of anatase added materials is also confirmed by the photos of the aged samples, which show a smaller size and distribution of sur-face defects (Fig. 7).

3.3. Accelerated photocatalytic activity

Rhodamine B degradation tests were performed on freshly prepared samples on which 2 ml of a solution of RhB with concentration 3×10^{-5} M were deposited and dried overnight. Results are reported in Fig. 8, where the dashed lines identify the photoactivity thresholds at 4 and 26 hours (i.e., $R_4 > 20\%$ and $R_{26} > 50\%$). TiO_2 containing samples can actually be considered photoactive according to [58], as they give extents of degradation $R_4 = 38\%$ and $R_{26} = 64\%$, respectively, while standard mortars do not satisfy the requirements.

Yet, as can be seen in Fig. 9, samples show limited photoactivity after environmental exposure, during which the material surface underwent extensive soiling. R_4 is reduced to approximately 20%, after one year of activity, while R_{26} falls slightly below 50%. Thus, an average reduction of approximately 20% of the degradation efficiency emerges from the RhB photodegradation tests on vertically exposed specimens. More relevant reductions, up to 65% of initial efficiency, were observed on more soiled specimens – e.g., horizontal ones. On the other hand, the loss in photoactivity after the second year of aging is not as significant as in the first year. Hence, it is possible to hypothesize that photoactivity is quickly reduced during the first months, following the same trend of L^* (Fig. 8 – limits for R_4 and R_{26} are given as dashed lines), and then stabilizes with asymptotic trend, as shown in Fig. 9. Standard samples did not show relevant photoactivity before exposure, and this remains unaltered after natural aging.

3.4. Accelerated cleaning

After observing the decay in photocatalytic activity with natural aging, a cleaning procedure was considered, consisting of alternating UV–Vis irradiation to decompose soil and light rinsing steps to

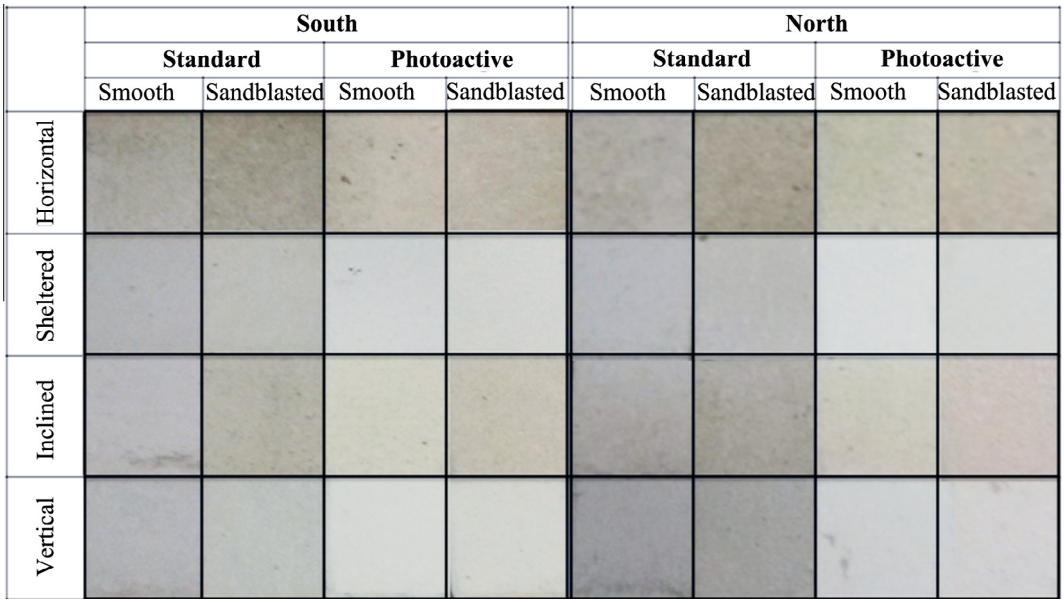

Fig. 7. Photograph of one sample per type of material and exposure conditions after two years of exposure. While all horizontal samples exhibit a clear surface soiling and deterioration, in the other inclinations this is only observed on standard specimens.

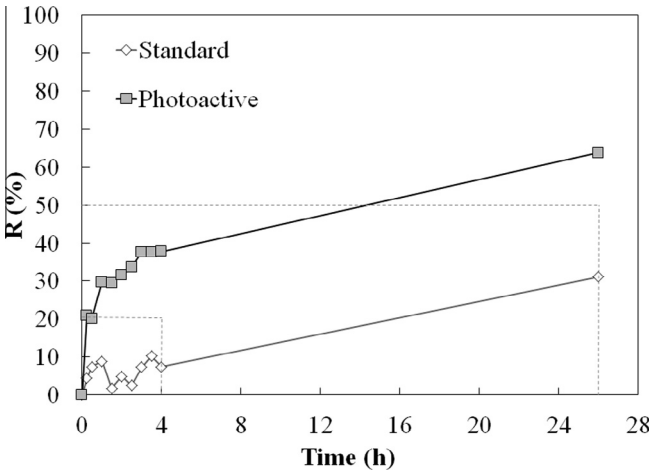

Fig. 8. *R*% (extent of degradation) of RhB solution, previously deposited and dried on samples, under UV–Vis irradiation on standard and photoactive samples.

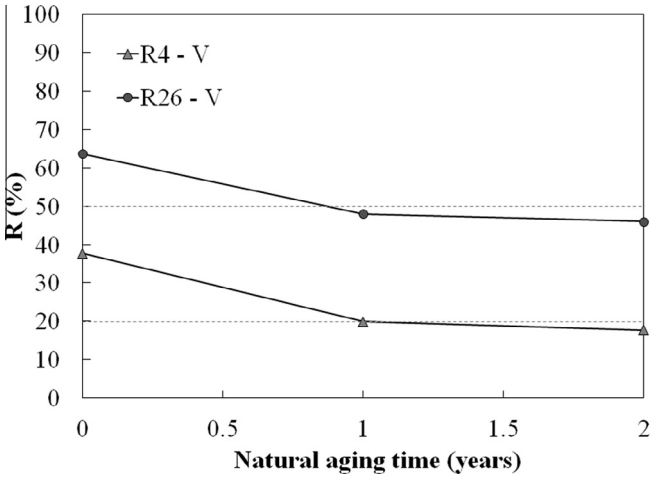

Fig. 9. R_4 and R_{26} for freshly prepared, 1 and 2 year naturally aged photoactive samples, exposed in vertical position.

remove the decomposition products and further contaminants. This was applied to horizontally exposed specimens, which pre-sented the worst color variations along with the worst photocat-alytic efficiency (R_{26} only 23%). Even though lightness recovery was similar on both photoactive and standard mortar (Fig. 10a), the former experienced higher lightness variation, in particular

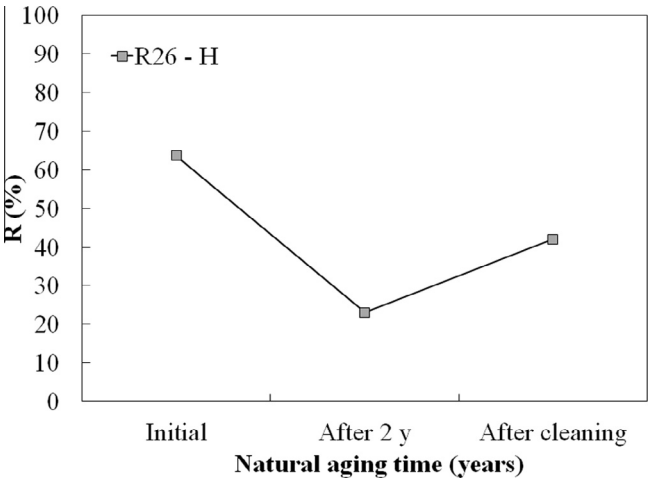

Fig. 11. R_{26} for RhB degradation on photoactive mortars: freshly prepared, after 2 years of natural aging in horizontal position and after accelerated cleaning.

when rinsed. This can be ascribed to the higher hydrophilicity of photoactive mortars, and to the actual onset of self-cleaning based on superhydrophilicity, which allows a better removal by water of the dirt accumulated onto the surface [41,42,45]. On the other hand, an even stronger effect can be observed on b^*, which represents yellow hues (Fig. 10b). Both mortars underwent an increase in b^* during natural aging due to the accumulation of particulate matter, but Δb^* was larger on photoactive samples: also the recovery of b^* was eventually larger on mortars containing TiO_2, again on account of the removal of yellowing soiling deposits and reaction products.

3.5. Photocatalytic activity after natural exposure and accelerated cleaning

After accelerated cleaning, photocatalytic degradation of RhB was tested again to observe possible recovery of photoactivity in TiO_2-containing mortars. Although the overall dye discoloration was lower than that observed in presence of freshly prepared samples, a significantly higher value (43%) was achieved compared with naturally aged specimens (23%), i.e., the same specimens before accelerated cleaning (Fig. 11). This means that the material effectively recovered almost 70% of its initial photocatalytic efficiency, which is an interesting result as it indicates that a periodic maintenance would restore values of photoactivity close to the initial ones.

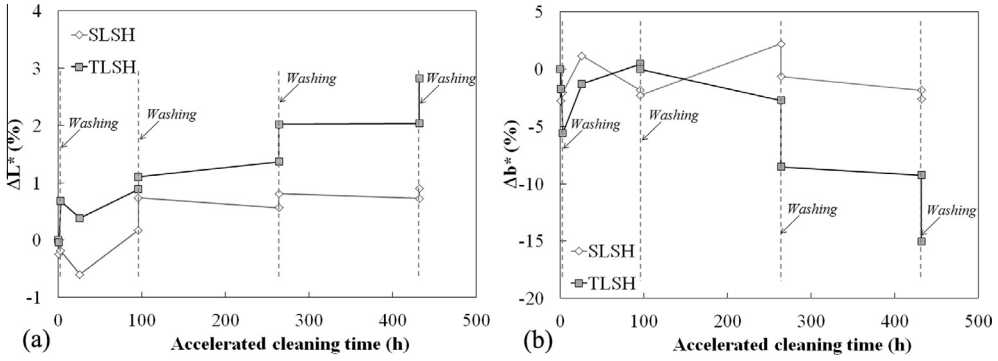

Fig. 10. Lightness variation ΔL^* (a) and b^* variation (b) recorded on mortars during artificial cleaning by UV–Vis irradiation and washing, starting from values reached at the end of natural exposure.

4. Conclusions

The depolluting and self-cleaning potential of photoactive building envelope materials has been object of several studies to preserve the aesthetics of façades and contribute to the mitigation of atmospheric pollution. Moreover, materials that could retain their initially high solar reflectance and thermal emittance can reduce the cooling needs of buildings, and cool roofs may mitigate urban heat islands. Products that rely on the photocatalytic properties of anatase are commercially available, but few studies assess their durability and long-term performance.

Herein was reported a two-year natural exposure in the urban environment of Milano of photoactive and non-photoactive fiber-reinforced mortars with different surface finishing, which are used for rain-screen or pre-cast thermally insulated façade panels, and we analyze the durability of the photocatalytic and self-cleaning properties over such long period of real environmental exposure under different orientations and inclinations.

All photoactive samples presented a lower or comparable lightness decrease than the standard non-photoactive mortars, but those facing north showed a more significant decrease in lightness, as they are less exposed to solar irradiation, which limits photoactivation. Moreover, anatase containing mortars, after aging, show higher surface homogeneity and integrity than standard samples, which is confirmed by a higher standard deviation of lightness and solar reflectance measurements on the latter ones.

Unlike standard mortars, TiO_2 containing samples can be classified as photoactive according to the standard UNI 11259, as they give extents of dye degradation $R_4 = 38\%$ and $R_{26} = 64\%$, respectively at 4 and 26 hours of irradiation. After 1 year of aging, R_4 is reduced to approximately 20%, while R_{26} falls slightly below 50%, yielding to an average degradation efficiency reduction of about 20% to 65%, depending on the degree of soiling. However, the loss in photoactivity after the second year is less marked than after the first year. Naturally aged samples were then subject to alternated cycles of UV–Vis irradiation and rinsing. After accelerated cleaning, photoactive mortars presented a higher initial lightness recovery than the standard ones, and they recovered almost 70% of their initial photocatalytic efficiency.

Acknowledgements

This work was in part funded by Politecnico di Milano & Agenzia delle Entrate (Italian Revenue Agency) with the project "Cinque per mille junior – Rivestimenti fluorurati avanzati per superfici edilizie ad alte prestazioni". The authors gratefully acknowledge the PIZ division of Zecca Prefabbricati S.p.A. for having supplied the materials tested in this experimental work. The authors thankfully acknowledge Cristina Tedeschi (Politecnico di Milano) for the porosimetry measurements.

References

[1] D. Spasiano, R. Marotta, S. Malato, P. Fernandez-Ibanez, I.D. Somma, Solar photocatalysis: materials, reactors, some commercial and pre-industrialized applications. A comprehensive approach, Appl. Catal. B Environ. 170 (2015) 90–123, http://dx.doi.org/10.1016/j.apcatb.2014.12.050.

[2] M. Radetić, Functionalization of textile materials with TiO_2 nanoparticles, J. Photochem. Photobiol. C Photochem. Rev. 16 (2013) 62–76, http://dx.doi.org/10.1016/j.jphotochemrev.2013.04.002.

[3] M.V. Diamanti, M.P. Pedeferri, Concrete, mortar and plaster using titanium dioxide nanoparticles: applications in pollution control, self-cleaning and photosterilisation, in: F. Pachego-Torgal, M. Diamanti, N. Nazari, C. Goran-Granqvist (Eds.), Nanotechnol. Eco-efficient Constr., Woodhead Publishing Ltd, Cambridge, UK, 2014, pp. 299–326.

[4] M. Baudys, J. Krýsa, M. Zlámal, A. Mills, Weathering tests of photocatalytic facade paints containing ZnO and TiO_2, Chem. Eng. J. 261 (2015) 83–87, http://dx.doi.org/10.1016/j.cej.2014.03.112.

[5] R. Levinson, P. Berdahl, H. Akbari, Solar spectral optical properties of pigments. Part II. Survey of common colorants, Sol. Energy Mater. Sol. Cells 89 (2005) 351–389, http://dx.doi.org/10.1016/j.solmat.2004.11.013.

[6] R. Levinson, P. Berdahl, H. Akbari, W. Miller, I. Joedicke, J. Reilly, et al., Methods of creating solar-reflective nonwhite surfaces and their application to residential roofing materials, Sol. Energy Mater. Sol. Cells 91 (2007) 304–314, http://dx.doi.org/10.1016/j.solmat.2006.06.062.

[7] A. Synnefa, M. Santamouris, K. Apostolakis, On the development, optical properties and thermal performance of cool colored coatings for the urban environment, Sol. Energy 81 (2007) 488–497, http://dx.doi.org/10.1016/j.solener.2006.08.005.

[8] E.S. Cozza, M. Alloisio, A. Comite, G. Di Tanna, S. Vicini, NIR-reflecting properties of new paints for energy-efficient buildings, Sol. Energy 116 (2015) 108–116, http://dx.doi.org/10.1016/j.solener.2015.04.004.

[9] F. Rossi, A.L. Pisello, A. Nicolini, M. Filipponi, M. Palombo, Analysis of retro-reflective surfaces for urban heat island mitigation: a new analytical model, Appl. Energy 114 (2014) 621–631, http://dx.doi.org/10.1016/j.apenergy.2013.10.038.

[10] F. Rossi, B. Castellani, A. Presciutti, E. Morini, M. Filipponi, A. Nicolini, et al., Retroreflective façades for urban heat island mitigation: experimental investigation and energy evaluations, Appl. Energy 145 (2015) 8–20, http://dx.doi.org/10.1016/j.apenergy.2015.01.129.

[11] R. Levinson, H. Akbari, Potential benefits of cool roofs on commercial buildings: conserving energy, saving money, and reducing emission of greenhouse gases and air pollutants, Energy Effic. 3 (2010) 53–109, http://dx.doi.org/10.1007/s12053-008-9038-2.

[12] A.L. Pisello, F. Rossi, F. Cotana, Summer and winter effect of innovative cool roof tiles on the dynamic thermal behavior of buildings, Energies 7 (2014) 2343–2361, http://dx.doi.org/10.3390/en7042343.

[13] M. Zinzi, S. Agnoli, Cool and green roofs. An energy and comfort comparison between passive cooling and mitigation urban heat island techniques for residential buildings in the Mediterranean region, Energy Build. 55 (2012) 66–76, http://dx.doi.org/10.1016/j.enbuild.2011.09.024.

[14] P.J. Rosado, D. Faulkner, D.P. Sullivan, R. Levinson, Measured temperature reductions and energy savings from a cool tile roof on a central California home, Energy Build. (2014), http://dx.doi.org/10.1016/j.enbuild.2014.04.024.

[15] M. Santamouris, Cooling the cities – a review of reflective and green roof mitigation technologies to fight heat island and improve comfort in urban environments, Sol. Energy 103 (2014) 682–703, http://dx.doi.org/10.1016/j.solener.2012.07.003.

[16] M. Santamouris, On the energy impact of urban heat island and global warming on buildings, Energy Build. 82 (2014) 100–113, http://dx.doi.org/10.1016/j.enbuild.2014.07.022.

[17] S. Magli, C. Lodi, L. Lombroso, A. Muscio, S. Teggi, Analysis of the urban heat island effects on building energy consumption, Int. J. Energy Environ. Eng. 6 (2014) 91–99, http://dx.doi.org/10.1007/s40095-014-0154-9.

[18] R. Paolini, M. Zinzi, T. Poli, E. Carnielo, A.G. Mainini, Effect of ageing on solar spectral reflectance of roofing membranes: natural exposure in Roma and Milano and the impact on the energy needs of commercial buildings, Energy Build. 84 (2014) 333–343, http://dx.doi.org/10.1016/j.enbuild.2014.08.008.

[19] M. Ichinose, T. Inoue, Y. Sakamoto, Long-term performance of high-reflectivity exterior panels, Build. Environ. 44 (2009) 1601–1608, http://dx.doi.org/10.1016/j.buildenv.2008.10.003.

[20] P. Berdahl, H. Akbari, R. Levinson, W.A. Miller, Weathering of roofing materials – an overview, Constr. Build. Mater. 22 (2008) 423–433, http://dx.doi.org/10.1016/j.conbuildmat.2006.10.015.

[21] M. Sleiman, G. Ban-Weiss, H.E. Gilbert, D. François, P. Berdahl, T.W. Kirchstetter, et al., Soiling of building envelope surfaces and its effect on solar reflectance. Part I. Analysis of roofing product databases, Sol. Energy Mater. Sol. Cells 95 (2011) 3385–3399, http://dx.doi.org/10.1016/j.solmat.2011.08.002.

[22] M.A. Shirakawa, A.P. Werle, C.C. Gaylarde, K. Loh, V.M. John, Fungal and phototroph growth on fiber cement roofs and its influence on solar reflectance in a tropical climate, Int. Biodeterior. Biodegrad. 95 (2014) 1–6, http://dx.doi.org/10.1016/j.ibiod.2013.12.003.

[23] H.K. Tanaca, C.M.R. Dias, C.C. Gaylarde, V.M. John, M.A. Shirakawa, Discoloration and fungal growth on three fiber cement formulations exposed in urban, rural and coastal zones, Build. Environ. 46 (2011) 324–330, http://dx.doi.org/10.1016/j.buildenv.2010.07.025.

[24] C. Ferrari, A. Gholizadeh Touchaei, M. Sleiman, A. Libbra, A. Muscio, C. Siligardi, et al., Effect of aging processes on solar reflectivity of clay roof tiles, Adv. Build. Energy Res. (2014) 1–13, http://dx.doi.org/10.1080/17512549.2014.890535.

[25] P. Berdahl, H. Akbari, L.S. Rose, Aging of reflective roofs: soot deposition, Appl. Opt. 41 (2002) 2355–2360.

[26] M. Sleiman, T.W. Kirchstetter, P. Berdahl, H.E. Gilbert, S. Quelen, L. Marlot, et al., Soiling of building envelope surfaces and its effect on solar reflectance. Part II. Development of an accelerated aging method for roofing materials, Sol. Energy Mater. Sol. Cells 122 (2014) 271–281, http://dx.doi.org/10.1016/j.solmat.2013.11.028.

[27] L. Graziani, E. Quagliarini, F. Bondioli, M. D'Orazio, Durability of self-cleaning TiO_2 coatings on fired clay brick façades: effects of UV exposure and wet & dry cycles, Build. Environ. 71 (2014) 193–203, http://dx.doi.org/10.1016/j.buildenv.2013.10.005.

[28] R. Pires, J. de Brito, B. Amaro, Statistical survey of the inspection, diagnosis and repair of painted rendered façades, Struct. Infrastruct. Eng. 11 (2014) 605–618, http://dx.doi.org/10.1080/15732479.2014.890233.

[29] M.V. Diamanti, R. Paolini, M. Zinzi, M. Ormellese, M. Fiori, M.P. Pedeferri, Self-cleaning ability and cooling effect of TiO_2-containing mortars, NSTI-Nanotech 2013, vol. 3, Washington, USA, 2013, pp. 716–719.

[30] K. Midtdal, B.P. Jelle, Self-cleaning glazing products: a state-of-the-art review and future research pathways, Sol. Energy Mater. Sol. Cells 109 (2013) 126–141, http://dx.doi.org/10.1016/j.solmat.2012.09.034.

[31] A. Chabas, T. Lombardo, H. Cachier, M.H. Pertuisot, K. Oikonomou, R. Falcone, et al., Behaviour of self-cleaning glass in urban atmosphere, Build. Environ. 43 (2008) 2124–2131, http://dx.doi.org/10.1016/j.buildenv.2007.12.008.

[32] G. Hüsken, M. Hunger, H.J.H. Brouwers, Experimental study of photocatalytic concrete products for air purification, Build. Environ. 44 (2009) 2463–2474, http://dx.doi.org/10.1016/j.buildenv.2009.04.010.

[33] M. Hunger, G. Hüsken, H.J.H. Brouwers, Photocatalytic degradation of air pollutants – from modeling to large scale application, Cem. Concr. Res. 40 (2010) 313–320, http://dx.doi.org/10.1016/j.cemconres.2009.09.013.

[34] T. Maggos, J.G. Bartzis, M. Liakou, C. Gobin, Photocatalytic degradation of NO_x gases using TiO_2-containing paint: a real scale study, J. Hazard. Mater. 146 (2007) 668–673, http://dx.doi.org/10.1016/j.jhazmat.2007.04.079.

[35] T. Maggos, A. Plassais, J.G. Bartzis, C. Vasilakos, N. Moussiopoulos, L. Bonafous, Photocatalytic degradation of NO_x in a pilot street canyon configuration using TiO_2-mortar panels, Environ. Monit. Assess. 136 (2008) 35–44, http://dx.doi.org/10.1007/s10661-007-9722-2.

[36] K. Liu, M. Cao, A. Fujishima, L. Jiang, Bio-inspired titanium dioxide materials with special wettability and their applications, Chem. Rev. 114 (2014) 10044–10094, http://dx.doi.org/10.1021/cr4006796.

[37] S. Ortelli, M. Blosi, C. Delpivo, D. Gardini, M. Dondi, I. Gualandi, et al., Multiple approach to test nano TiO_2 photo-activity, J. Photochem. Photobiol. A Chem. 292 (2014) 26–33, http://dx.doi.org/10.1016/j.jphotochem.2014.07.006.

[38] O. Carp, C.L. Huisman, A. Reller, Photoinduced reactivity of titanium dioxide, Prog. Solid State Chem. 32 (2004) 33–177, http://dx.doi.org/10.1016/j.progsolidstchem.2004.08.001.

[39] M.R. Hoffmann, S.T. Martin, W. Choi, D.W. Bahnemann, Environmental applications of semiconductor photocatalysis, Chem. Rev. 95 (1995) 69–96, http://dx.doi.org/10.1021/cr00033a004.

[40] M.V. Diamanti, B. Del Curto, M. Ormellese, M.P. Pedeferri, Photocatalytic and self-cleaning activity of colored mortars containing TiO_2, Constr. Build. Mater. 46 (2013) 167–174, http://dx.doi.org/10.1016/j.conbuildmat.2013.04.038.

[41] V.A. Ganesh, H.K. Raut, A.S. Nair, S. Ramakrishna, A review on self-cleaning coatings, J. Mater. Chem. 21 (2011) 16304, http://dx.doi.org/10.1039/c1jm12523k.

[42] R. Wang, K. Hashimoto, A. Fujishima, M. Chikuni, E. Kojima, A. Kitamura, et al., Light-induced amphiphilic surfaces, Nature 388 (1997) 431–432.

[43] M.V. Diamanti, K.R. Gadelrab, M.P. Pedeferri, M. Stefancich, S.O. Pehkonen, M. Chiesa, Nanoscale investigation of photoinduced hydrophilicity variations in anatase and rutile nanopowders, Langmuir 29 (2013) 14512–14518, http://dx.doi.org/10.1021/la4034723.

[44] F. Pacheco-Torgal, S. Jalali, Nanotechnology: advantages and drawbacks in the field of construction and building materials, Constr. Build. Mater. 25 (2011) 582–590, http://dx.doi.org/10.1016/j.conbuildmat.2010.07.009.

[45] A. Fujishima, X. Zhang, Titanium dioxide photocatalysis: present situation and future approaches, Comptes Rendus Chim. 9 (2006) 750–760, http://dx.doi.org/10.1016/j.crci.2005.02.055.

[46] S. De Niederhäusern, M. Bondi, F. Bondioli, Self-cleaning and antibacteric ceramic tile surface, Int. J. Appl. Ceram. Technol. 10 (2013) 949–956, http://dx.doi.org/10.1111/j.1744-7402.2012.02801.x.

[47] J. Chen, C. Poon, Photocatalytic construction and building materials: from fundamentals to applications, Build. Environ. 44 (2009) 1899–1906, http://dx.doi.org/10.1016/j.buildenv.2009.01.002.

[48] A. Maury-Ramirez, K. Demeestere, N. De Belie, Photocatalytic activity of titanium dioxide nanoparticle coatings applied on autoclaved aerated concrete: effect of weathering on coating physical characteristics and gaseous toluene removal, J. Hazard. Mater. 211–212 (2012) 218–225, http://dx.doi.org/10.1016/j.jhazmat.2011.12.037.

[49] C. Pirola, D.C. Boffito, S. Vitali, C.L. Bianchi, Photocatalytic coatings for building industry: study of 1 year of activity in the NO_x degradation, J. Coatings Technol. Res. 9 (2011) 453–458, http://dx.doi.org/10.1007/s11998-011-9381-7.

[50] M.M. Hassan, H. Dylla, L.N. Mohammad, T. Rupnow, Evaluation of the durability of titanium dioxide photocatalyst coating for concrete pavement, Constr. Build. Mater. 24 (2010) 1456–1461, http://dx.doi.org/10.1016/j.conbuildmat.2010.01.009.

[51] M.V. Diamanti, M.F. Brunella, M.P. Pedeferri, C. Pirotta, P. Manzocchi, S. Curtoni, Self-cleaning and antipolluting properties of TiO_2-containing cementitious materials, NSTI Nanotech, Santa Clara, California, USA, 2007, pp. 1–5.

[52] S.H. Zhang, D. Tanadi, W. Li, Effect of photocatalyst TiO_2 on workability, strength and self-cleaning efficiency of mortars for applications in tropical environment, 35th Conf. Our World Concr. Struct. 2010, Singapore, 2010.

[53] M.V. Diamanti, M. Ormellese, M. Pedeferri, Characterization of photocatalytic and superhydrophilic properties of mortars containing titanium dioxide, Cem. Concr. Res. 38 (2008) 1349–1353, http://dx.doi.org/10.1016/j.cemconres.2008.07.003.

[54] ISO. ISO 9050 – glass in building – determination of light transmittance, solar direct transmittance, total solar energy transmittance, ultraviolet transmittance and related glazing factors, 2003.

[55] I.K. Konstantinou, T.A. Albanis, TiO_2-assisted photocatalytic degradation of azo dyes in aqueous solution: kinetic and mechanistic investigations, Appl. Catal. B Environ. 49 (2004) 1–14, http://dx.doi.org/10.1016/j.apcatb.2003.11.010.

[56] U.G. Akpan, B.H. Hameed, Parameters affecting the photocatalytic degradation of dyes using TiO_2-based photocatalysts: a review, J. Hazard. Mater. 170 (2009) 520–529, http://dx.doi.org/10.1016/j.jhazmat.2009.05.039.

[57] D. Ollis, Kinetics of photocatalyzed film removal on self-cleaning surfaces: simple configurations and useful models, Appl. Catal. B Environ. 99 (2010) 478–484, http://dx.doi.org/10.1016/j.apcatb.2010.06.029.

[58] UNI. UNI 11259. Determination of the Photocatalytic Activity of Hydraulic Binders. Rodammina Test Method, 2008.

[59] R.A. Shah, J. Pitroda, Effect of water absorption and sorptivity on durability of pozzocrete mortar, Int. J. Emerg. Sci. Eng. 1 (2013) 73–77.

[60] A. Nazari, S. Riahi, The effects of TiO_2 nanoparticles on properties of binary blended concrete, J. Compos. Mater. 45 (2010) 1181–1188, http://dx.doi.org/10.1177/0021998310378910.

[61] J. Cai, B. Yu, A discussion of the effect of tortuosity on the capillary imbibition in porous media, Transp. Porous Media 89 (2011) 251–263, http://dx.doi.org/10.1007/s11242-011-9767-0.

[62] L.F. Jacques, Accelerated and outdoor/natural exposure testing of coatings, Prog. Polym. Sci. 25 (2000) 1337–1362, http://dx.doi.org/10.1016/S0079-6700(1)00030-7.

[63] L. Peruchon, E. Puzenat, A. Girard-Egrot, L. Blum, J.M. Herrmann, C. Guillard, Characterization of self-cleaning glasses using Langmuir–Blodgett technique to control thickness of stearic acid multilayers. Importance of spectral emission to define standard test, J. Photochem. Photobiol. A Chem. 197 (2008) 170–176, http://dx.doi.org/10.1016/j.jphotochem.2007.12.033.